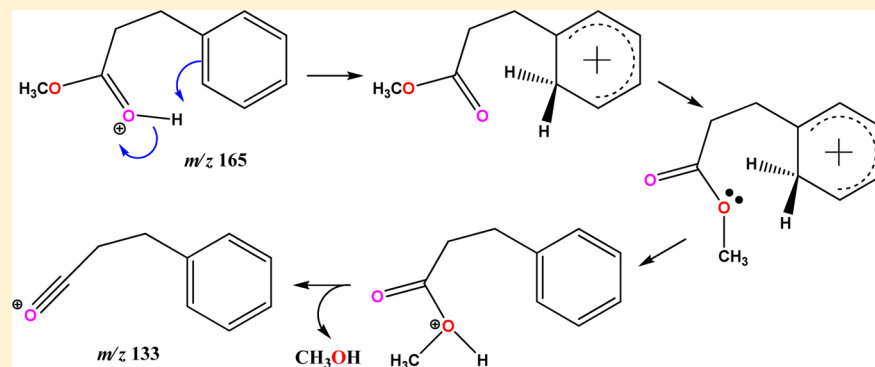


# Ambulation of Incipient Proton during Gas-Phase Dissociation of Protonated Alkyl Dihydrocinnamates

Sihang Xu, Yong Zhang, Ramu Errabelli, and Athula B. Attygalle\*

Center for Mass Spectrometry, Department of Chemistry, Chemical Biology, and Biomedical Engineering, Stevens Institute of Technology, Hoboken, New Jersey 07030, United States

 Supporting Information



**ABSTRACT:** Upon activation in the gas phase, protonated alkyl dihydrocinnamates undergo an alcohol loss. However, the mechanism followed is not a simple removal of an alkanol molecule after a protonation on the alkoxy group. The mass spectrum of the  $m/z$  166 ion for deuteron-charged methyl dihydrocinnamate showed two peaks of 1:5 intensity ratio at  $m/z$  133 and 134 to confirm that the incipient proton is mobile. The proton initially attached to the carbonyl group migrates to the ring and randomizes before a subsequent transfer of one of the ring protons to the alkoxy group for the concomitant alcohol elimination. Moreover, protonated methyl dihydrocinnamate undergoes more than one H/D exchange. The spectra recorded from  $m/z$  167 and 168 ions obtained for *di*- and *tri*-deutero isotopologues showed peak pairs at  $m/z$  134, 135 and 135, 136, at 1:2 and 1:1 intensity ratios, respectively, confirming the benzenium ion intermediate achieves complete randomization before the proton transfer. Additionally, protonated higher esters of alkyl dihydrocinnamates undergo a cleavage of the O–CH<sub>2</sub> bond to form an ion/neutral complex, which, upon activation, dissociates generating a carbénium ion and dihydrocinnamic acid, or rearranges to generate protonated dihydrocinnamic acid and an alkene by a nonspecific proton transfer.

## INTRODUCTION

Dihydrocinnamic acid and its derivatives are key synthetic intermediates for several pharmaceuticals and biologically relevant compounds.<sup>1</sup> Moreover, dihydrocinnamate esters are fragrant substances widely used in the cosmetic industry. In addition, they are employed in the food industry as flavor preservatives of frozen foods. Mass spectrometry is one of the methods available for detection and quantification of dihydrocinnamates. However, to carry out a mass spectrometric analysis, gaseous ions must first be generated from dihydrocinnamates. Besides traditional electron ionization, electrospray ionization (ESI) is one of the most widely deployed techniques for gas-phase ion generation from a variety of analytes. However, ESI is not an efficient technique for ionizing compounds of low proton affinity such as esters. The recently described “Helium Plasma Ionization (HePI),”<sup>2,3</sup> and DART<sup>4</sup> methods, on the other hand, are more suitable for generating gaseous ions from esters. Under HePI conditions, abundant ions are generated for the respective protonated species of alkyl dihydrocinnamates.

To obtain structural information from gaseous ions, they are usually mass selected by tandem mass spectrometry and subjected to collision-induced dissociation (CID). At first glance, the CID spectra of protonated esters appear simple.<sup>5</sup> However, the interpretation of CID spectra is not always straightforward because many rearrangements take place during fragmentation. Three major fragmentation pathways have been proposed to rationalize gas-phase dissociation reactions of protonated esters.<sup>5</sup> A loss of an alcohol molecule by the cleavage of the bond between the alkoxy and carbonyl moieties to generate an acylium cation is one of the primary fragmentation pathways proposed for protonated esters. However, a secondary pathway, in which an alkene molecule is eliminated to form the protonated acid, appears to take precedence for many esters with long-chain alkyl groups. In the third mechanism, the protonated ester eliminates the acid to generate a carbénium ion. Although protonated alkyl dihydrocinnamates lose an alcohol as envisaged by the first

Received: June 19, 2015

Published: September 2, 2015

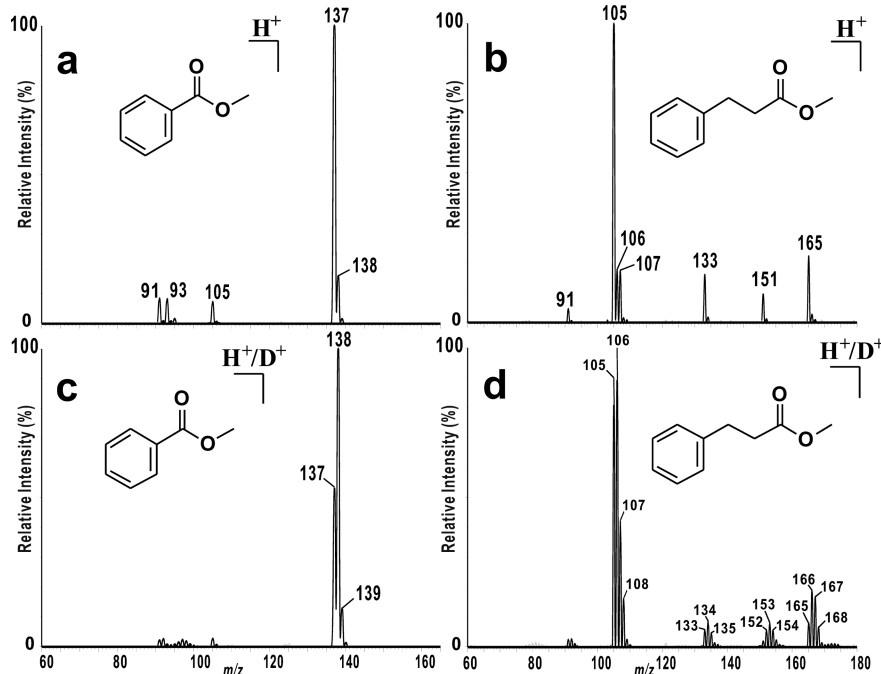


**Figure 1.** Unit-resolution HePI mass spectra recorded under atmospheric positive-ion-generating conditions from methyl benzoate (a), and methyl dihydrocinnamate (b). (c and d) Spectra recorded under similar conditions from methyl benzoate and methyl dihydrocinnamate, respectively, from samples exposed to atmospheric air saturated with D<sub>2</sub>O in an enclosed source.

mechanism, herein we demonstrate that it is not a single-step reaction. Our results from detailed deuterium-exchange experiments show that the incipient proton that attaches to the carbonyl group is mobile, and it ambulates to the phenyl ring before migrating to the alkoxy oxygen atom for the subsequent alcohol loss. At least for peptides and amino acid derivatives, it is accepted that, upon ion activation, the charge-imparting proton migrates to several protonation sites and triggers charge-directed bond cleavages.<sup>6,7</sup> In the present study, tandem mass spectrometry of several <sup>18</sup>O- and <sup>2</sup>H-labeled compounds, along with computational methods, was used to follow the charge-directed gas-phase fragmentation mechanisms of protonated alkyl dihydrocinnamates.

## RESULTS AND DISCUSSION

Electrospray-ionization spectra recorded from esters often do not show peaks for the molecular species because protonated esters undergo rapid fragmentation, even under the mildest ion activation conditions. In contrast, the HePI procedure, which is a very soft ionization technique, provides a convenient method for generating protonated esters.<sup>3</sup> For example, methyl benzoate generates abundant ions under positive-ion HePI conditions, and its spectrum shows an intense peak at *m/z* 137 for the protonated species (Figure 1a).

Analogously, esters of dihydrocinnamic acid also yield abundant protonated molecules when subjected to HePI. For example, the spectrum recorded from methyl dihydrocinnamate showed a significant peak *m/z* 165 for the protonated species (Figure 1b). However, this *m/z* 165 ion is very fragile: it undergoes fragmentation upon minimal activation. The fragmentation spectrum recorded from the mass-isolated *m/z* 165 ion showed a major peak at *m/z* 133 for a neutral loss of a 32-Da molecule (Figure 2a). Clearly, this neutral loss represents the elimination of methanol. The spectrum recorded from the *m/z* 167 ion generated from methyl [carbonyl-<sup>18</sup>O]dihydro-

cinnamate showed a peak specifically at *m/z* 133, which confirmed that the carbonyl oxygen atom is not removed when methanol is eliminated from protonated methyl dihydrocinnamate (Figure 2b). Analogously, the spectrum recorded from the *m/z* 168 ion generated from [3,3,3-<sup>2</sup>H<sub>3</sub>]methyl dihydrocinnamate established that the deuterons in the trideuteriomethyl group remain intact, without any scrambling, during the elimination reaction (Figure 2c). Based on these observations, one may presume the fragmentation pathway to be simple: an initial protonation on the oxygen atom of the methoxy group, followed by a direct elimination of a methanol molecule. However, a detailed experimental study revealed that the mechanism is more complex, and the incipient proton ambulates to the phenyl ring before the alcohol molecule is eventually eliminated.

The first evidence for this intricate phenomenon came from in-source H/D exchange experiments. We recently showed the efficacy of in-source H/D exchange experiments for structural investigations.<sup>3</sup> The spectrum recorded from methyl benzoate exposed to D<sub>2</sub>O vapor in the source showed a dramatic intensity increase of the *m/z* 138 peak (Figure 1c), which indicated that protonated methyl benzoate undergoes predominantly one H/D exchange under these experimental conditions. In contrast, the spectrum recorded from methyl dihydrocinnamate under similar conditions showed intensity increases of many peaks beyond that of *m/z* 165 (Figure 1d). In other words, protonated methyl dihydrocinnamate rapidly undergoes more than one D/H exchange, and the respective peak intensity increases are higher than those expected due to the presence of <sup>13</sup>C isotopologues. The CID spectrum recorded from the *m/z* 168 ion for protonated [3,3,3-<sup>2</sup>H<sub>3</sub>]methyl dihydrocinnamate, which showed peaks at *m/z* 91, 105, and 133, confirmed that none of these fragment ions acquire any deuterium labeling from the trideuteriomethyl group during fragmentation (Figure 2c). In other words, all the deuterium atoms in the deuteriomethyl

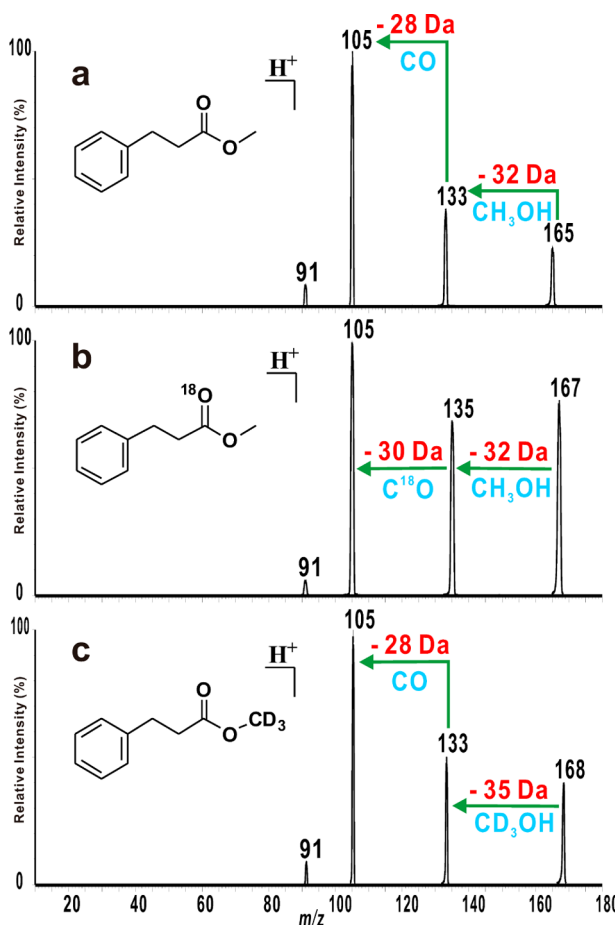


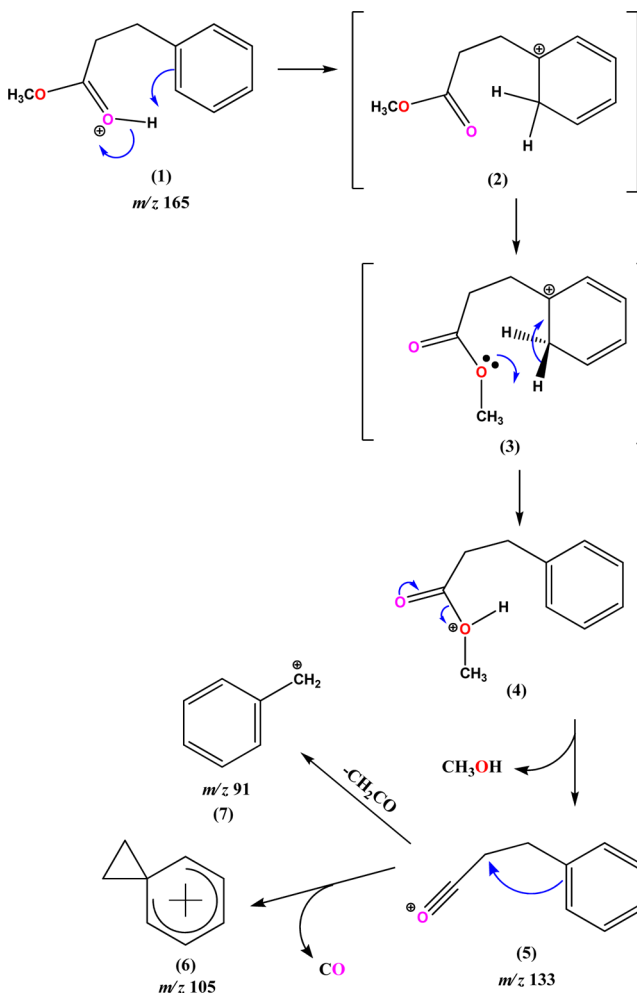
**Figure 2.** Unit-resolution product ion spectrum of  $m/z$  165 [ $(\text{M} + \text{H})^+$ ] ion generated from methyl dihydrocinnamate (a),  $m/z$  167 of methyl [carbonyl-<sup>18</sup>O]dihydrocinnamate (b), and  $m/z$  168 [ $(\text{M} + \text{H})^+$ ] ion of [3,3,3-<sup>2</sup>H<sub>3</sub>]methyl dihydrocinnamate (c), recorded at a laboratory-frame collision energy settings of 17 eV on a tandem quadrupole mass spectrometer (all parameters, including collision gas pressure and skimmer voltage, were identical).

group are eliminated in the form of  $\text{CD}_3\text{OH}$  when the  $m/z$  133 ion is formed from the precursor  $m/z$  168 ion.

In order to figure out the fate of the incipient charge-imparting proton during the fragmentation of protonated methyl dihydrocinnamate, we recorded fragment ion spectra of mono-, di-, and tri-deutero isotopologues of methyl dihydrocinnamate generated in the ion source by in-source D/H exchanges. To start with, the spectrum recorded with the  $m/z$  166 ion (Figure 3a) showed that the charge-imparting deuteron is not removed exclusively as  $\text{CH}_3\text{OD}$  during the elimination because the spectrum showed two peaks at  $m/z$  133 (loss of  $\text{CH}_3\text{OD}$ ) and  $m/z$  134 (loss of  $\text{CH}_3\text{OH}$ ) at an intensity ratio of 1:5. In other words, the simplest mechanism that could be envisaged, which is a direct protonation on the methoxy group, followed by a straightforward elimination of a methanol molecule, is not the predominant mechanism that is followed during the methanol elimination. Evidently, the ring hydrogen atoms also serve as a source of the hydrogen atom that is removed during the methanol loss. Furthermore, the intensity ratio of  $m/z$  134 and 135 peaks in Figure 3b is nearly 1:2, and that of  $m/z$  135 and 136 peaks in Figure 3c is approximately 1:1, which confirmed that the incipient proton and the five ring protons stand nearly the same probability of supplying the proton required for the methanol

loss. To rationalize these experimental observations, we propose the fragmentation mechanism given in Scheme 1. Our results

**Scheme 1. Proposed Mechanism for the Loss of Methanol from Protonated Methyl Dihydrocinnamate**



confirmed that the charge-imparting proton on the carbonyl group (1), once transferred to the ring, undergoes a complete randomization before one of the ring protons of the benzenium ion intermediate (2) formed in this way is transferred to the methoxy group. Rapid randomization by proton transfer in benzenium ions is a well-known phenomenon.<sup>8</sup>

To further support the proposed fragmentation mechanisms, we scrutinized the potential protonation sites of  $\text{PhCH}_2\text{CH}_2\text{CO}_2\text{CH}_3$  by computational methods. The calculated Gibbs free energies of each protonated molecule with respect to that of the lowest-energy carbonyl-oxygen-protonated congener are shown in Table 1.<sup>9</sup> The optimized structures obtained are depicted in Figure 4. According to our computational results, the carbonyl oxygen is the most favorable site to accept the incipient proton. Computations also showed that, once protonated, the carboxylate group is poised closer to the phenyl ring to maximize interactions (1; Figure 4). The initial addition of the proton to the carbonyl oxygen atom elongates the C=O double bond to 1.283 Å with concomitant shortening of the carbonyl-carbon and alkoxy-oxygen bond to 1.273 Å. In contrast, a protonation at the alkoxy oxygen site is dissociative (4). Such a protonation elongates the bond to 1.585 Å and enforces the immediate

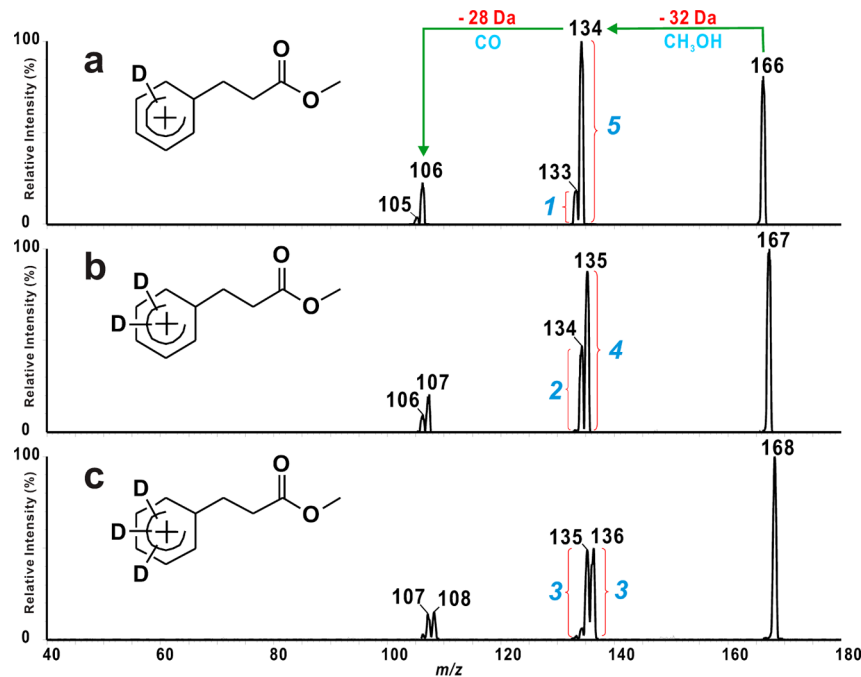


**Figure 3.** Product ion spectra of  $m/z$  166 (a), 167 (b), and 168 (c) ions generated by in-source D/H exchanges from methyl dihydrocinnamate exposed to  $\text{D}_2\text{O}$  vapor (collision energy = 6 eV).

**Table 1.** Relative Gibbs Free Energies (in kcal/mol) of Methyl Dihydrocinnamate and Methyl Benzoate Protonated at Different Sites, Computed for 298.15 K and 1 atm by the Density Functional Theory Method B3LYP Using a 6-311++G(2d,2p) Basis Set

	Carbonyl	Alkoxy	Ph-1 ( <i>ipso</i> )	Ph-2 ( <i>ortho</i> )	Ph-3 ( <i>meta</i> )	Ph-4 ( <i>para</i> )
$\text{PhCH}_2\text{CH}_2\text{CO}_2\text{Me}$	0.00	17.64	19.64	10.78	15.60	11.15
$\text{PhCO}_2\text{Me}$	0.00	17.40	27.78	23.41	23.66	24.38

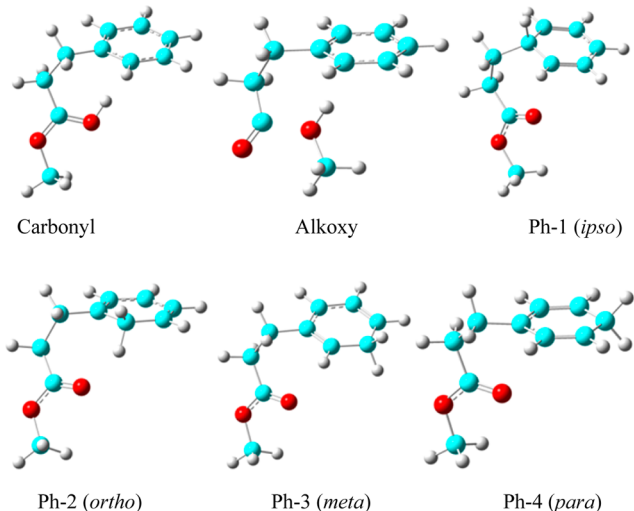


**Figure 4.** Optimized structures computed for the six protonation sites of  $\text{PhCH}_2\text{CH}_2\text{CO}_2\text{Me}$ .

dissociation of the bond between the alkoxy oxygen atom and the carbonyl carbon. It is interesting to note that, among the four possible protonations on the phenyl ring, not only is an *ipso* protonation less favorable than a proton addition to the alkoxy oxygen but also such an addition disrupts the planarity of the  $\text{PhCH}_2$  moiety (Ph-1 in Figure 4). For the other three possible ring protonation sites, the protonation preference follows the order *ortho* > *para* > *meta*.

An analogous calculation showed that the lowest energy protonation site for methyl benzoate is also the carbonyl oxygen, but the second-lowest-energy site is the alkoxy oxygen (Table 1). Thus, it is not surprising that protonated methyl benzoate is more sluggish to H/D exchanges because a protonation at any ring site of the molecule increases its relative energy to a higher level than that predicted for the alkoxy protonation (Table 1). On the other hand, for methyl dihydrocinnamate, a transfer from the protonated carbonyl group to the phenyl ring is a more favorable process than a transfer to the alkoxy group. Our computational results (Table 1) show the *ortho* position to be the most preferred ring protonation site. In addition, the Gibbs free energy barrier for the proton transfer from the carbonyl oxygen site to the ring *ortho* position via the seven-member transition state  $\text{TS}_{1-2}$  is relatively low (11.45 kcal/mol) (1 → 2 Scheme 1; Figure S).<sup>10</sup>

Once the ring is protonated, the benzenium ion formed may undergo rapid interactions with ambient water (or  $\text{D}_2\text{O}$ ) in the ion source. The benzenium ion is well-known to undergo rapid H/D exchanges with  $\text{D}_2\text{O}$ .<sup>11–14</sup> The product-ion spectrum recorded from the  $m/z$  168 ion for the *tri*-deutero isotopologue of protonated methyl dihydrocinnamate suggested that complete D/H scrambling occurs rapidly to reach a steady state, once the phenyl ring is charged (Figure 3c). Upon activation, the methoxy group in intermediate 2 pivots to form another intermediate (3), in which the methoxy group is closer to the *ortho* position.<sup>15</sup> A proton is then transferred from the benzenium intermediate 3 to the methoxy oxygen (3 → 4; Scheme 1).<sup>16</sup> The protonation of the methoxy oxygen is dissociative, leading to the immediate cleavage of the bond between this oxygen and the carbonyl

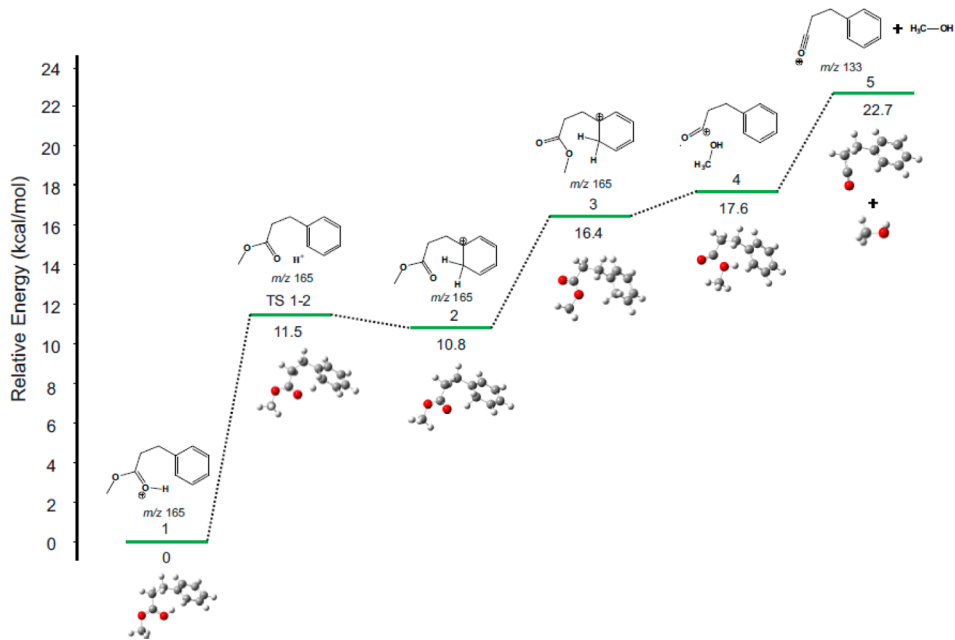


**Figure 5.** Relative Gibbs free energies (in kcal/mol computed for 298.15 K and 1 atm by the density functional theory method B3LYP using a 6-311+G(2d,2p) basis set) and structures of energy-optimized product ions and transition states associated with the methanol loss from protonated methyl dihydrocinnamate (1).

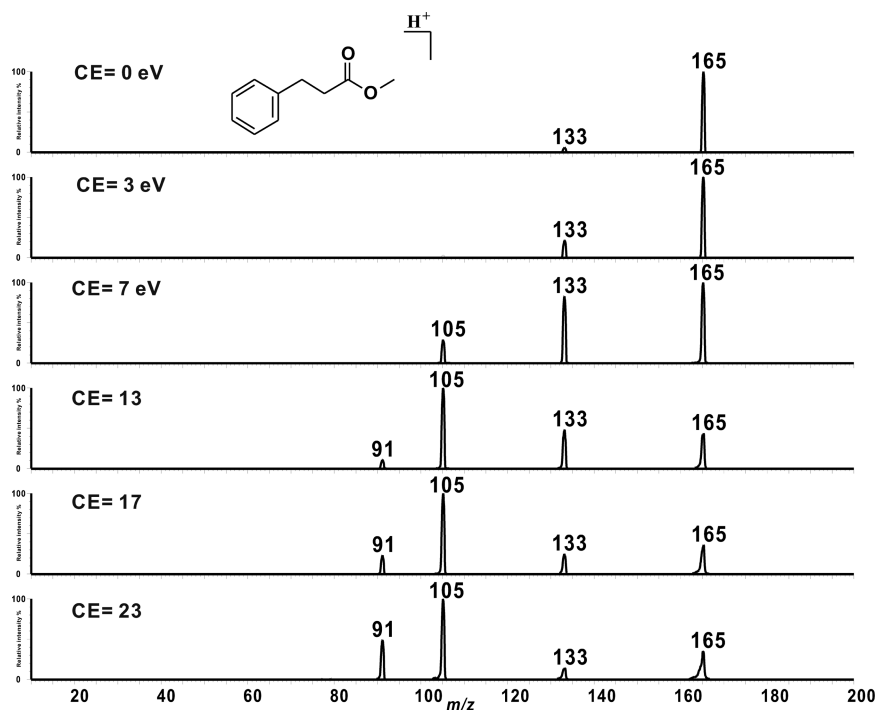


**Figure 6.** Product-ion spectra recorded from the  $m/z$  165  $[M + H]^+$  ion generated from methyl dihydrocinnamate, recorded at collision energy settings ranging from 0 to 23 eV (all parameters, including collision gas pressure and skimmer voltage, were identical).

carbon as evidenced by the concomitant elongation of the bond length to 1.585 Å. Presumably, the loss of the alcohol moiety from protonated higher esters of dihydrocinnamic acid occurs in an analogous manner.

Furthermore, the product-ion spectrum recorded from the  $m/z$  169 ion generated from methyl  $[2,2,3,3-^2\text{H}_4]$  dihydrocinnamate showed distinct peaks at  $m/z$  137 and 109 to confirm that side-chain deuterium atoms do not scramble with the ring hydrogens of the benzenium intermediate during the trans-

formations illustrated in Scheme 1 (Supporting Information Figure S1).

The (3-phenylpropylidene)oxonium ion ( $m/z$  133; 5) produced by alcohol elimination subsequently loses either a molecule of carbon monoxide to form the spiro[2,5]octanyl cation ( $m/z$  105; ethylene benzenium ion, 6) or a molecule of ketene to form the benzyl cation (7; Scheme 1). According to our experimental results, the formation of the  $m/z$  105 ion is favored over that of the  $m/z$  91 ion (Figure 6), which is congruent with

the Gibbs free reaction energy calculations. The fragmentation of the  $m/z$  133 ion to generate the  $m/z$  105 ion and carbon monoxide requires only 1.47 kcal/mol, while the energy demand for the formation of the  $m/z$  91 ion and ketene is 11.47 kcal/mol. The formation of the ethylene benzenium ion has been implicated not only in the gas phase<sup>17</sup> but also in solution.<sup>18</sup> Upon activation, the  $m/z$  105 ion fragments further by an elimination of a dihydrogen molecule or an acetylene molecule (see Supporting Information Figure S2).

Fragmentation pathways of protonated esters of dihydrocinnamates made with higher alcohols were also investigated. Although the fragmentation pattern of the protonated ethyl derivative was closely similar to that of the methyl ester, a low-intensity peak at  $m/z$  151 indicated a loss of an ethylene molecule from the protonated species (Figure 7a; see also Supporting

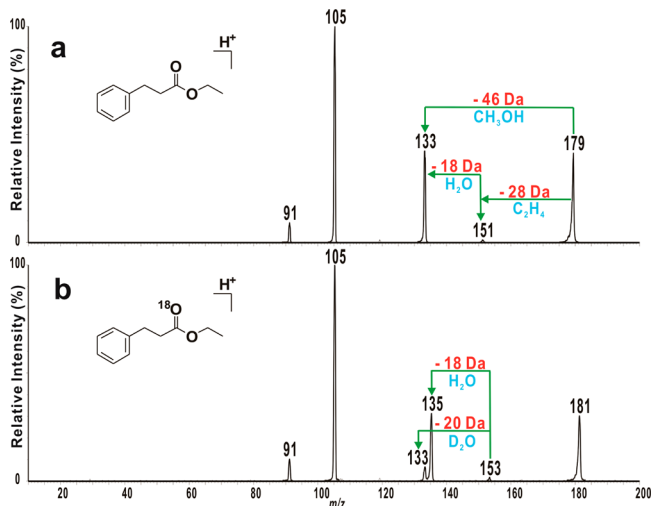
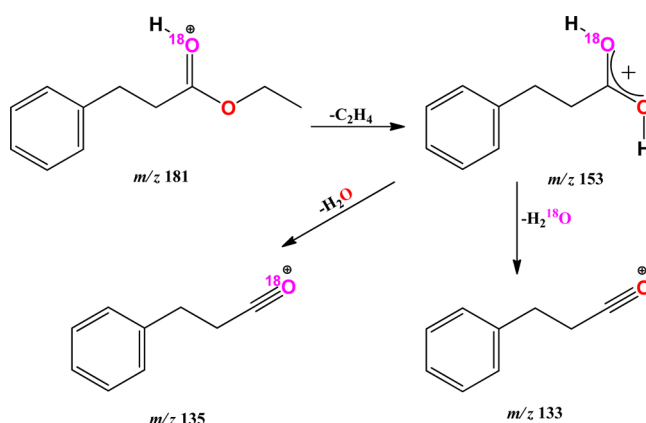


**Figure 7.** Product-ion spectra of  $m/z$  179 ion of protonated ethyl dihydrocinnamate (a) and  $m/z$  181 ion of protonated ethyl [carbonyl- $^{18}\text{O}$ ]dihydrocinnamate (b), recorded at a collision energy setting of 17 eV.

Information Figure S3). However, the spectrum recorded from protonated ethyl [carbonyl- $^{18}\text{O}$ ]dihydrocinnamate showed two peaks at  $m/z$  133 and 135 at an intensity ratio of 1:5 (Figure 7b). In contrast to the formation of the  $m/z$  133 ion from protonated methyl dihydrocinnamate by a direct methanol loss, which was confirmed by the complete retention of the carbonyl oxygen, the spectrum of protonated ethyl [carbonyl- $^{18}\text{O}$ ]dihydrocinnamate indicated that the  $m/z$  133 ion from the ethyl ester can be formed either with or, to a small extent, without the retention of the carbonyl oxygen. The direct loss of ethanol generates the  $m/z$  135 ion, which is the favored process. The results confirmed that the  $m/z$  133 and 135 ions are generated to a small extent also from the  $m/z$  153 ion by a water loss (Scheme 2). The  $m/z$  153 ion, which represents protonated [ $^{18}\text{O}$ ]dihydrocinnamic acid, can lose either  $\text{H}_2\text{O}$  or  $\text{H}_2^{18}\text{O}$  with nearly equal ease, if we disregard the small contribution due to the kinetic isotope effect.

The contribution of this additional mechanism to the formation of the  $m/z$  133 ion was confirmed by the results obtained from isotopologues generated by H/D-exchange of ethyl dihydrocinnamate. The fragment-ion spectra of *mono*-, *di*-, and *tri*-deutero isotopologues of ethyl dihydrocinnamate generated by in-source D/H exchange are illustrated in Figure 8. The intensity of the  $m/z$  135 peak is nearly double that of the  $m/z$  136 peak in Figure 8d, which indicates that the charge-

**Scheme 2. Proposed Mechanism for the Loss of Ethylene and Water from Protonated Ethyl Dihydrocinnamate**



imparting deuterium tends to undergo removal as  $\text{C}_2\text{H}_5\text{OD}$  more readily because of the additional contribution of this alkene-plus-water loss mechanism. We may recall that the intensities of the  $m/z$  135 and 136 peaks recorded from *tri*-deutero isotopologues of protonated methyl dihydrocinnamate are nearly equal (Figure 3c). In summary, we can conclude that the intensity ratio of the  $m/z$  133 to 135 peaks (Figure 7) provides a semiquantitative estimate of the relative contributions of the two mechanisms to the formation of the (3-phenylpropylidene)oxonium ( $m/z$  133; 5) ion in the ethyl ester (see also Supporting Information Figure S4 for an application).

The contribution from the alkene loss becomes more pronounced as the size of the alcohol residue of dihydrocinnamates increases, which is indicated by the increase of the intensity of the  $m/z$  151 peak as the length of the alkyl group increases (Figure 9). For example, the  $m/z$  151 peak for a propene loss is very prominent in the spectra of protonated *n*-propyl and isopropyl dihydrocinnamates (Figure 10). In fact, *n*-propyl and isopropyl dihydrocinnamate can be distinguished on the basis of their product-ion spectra because the latter eliminates a molecule of propene more readily. In general, isopropyl dihydrocinnamate is more susceptible to fragmentation than its *n*-propyl congener. We propose that upon protonation the O—alkyl bond elongates and undergoes a heterolytic cleavage to form an ion/neutral complex (INC). Direct dissociation of the INC can generate a propyl cation and dihydrocinnamic acid. However, it has been postulated that, before an ion-neutral-complex dissociates, a less stable alkyl cation within the complex can undergo rapid rearrangements by 1,2-hydride and alkydene shifts to a more stable carbenium ion or a proton-bridged complex.<sup>19–23</sup> Thus, it is likely that within the INC generated from protonated *n*-propyl dihydrocinnamate, the *n*-propyl cation rearranges to an isopropyl cation before the separation occurs. Because such a rearrangement is not necessary for the isopropyl cation within the INC of protonated isopropyl dihydrocinnamate, the elimination of propene from this complex does not require much collisional activation (see relative intensity profiles in Supporting Information Figure S5).

Analogous results were obtained from isomeric butyl dihydrocinnamates. Although the spectra were qualitatively similar (Figure 11), the peak-intensity profiles recorded by varying collision energy showed that each isomer can be distinguished by the propensity of the formation of specific product ions (see Supporting Information Figure S6). Evidently, there are several competitive fragmentation pathways. The initial

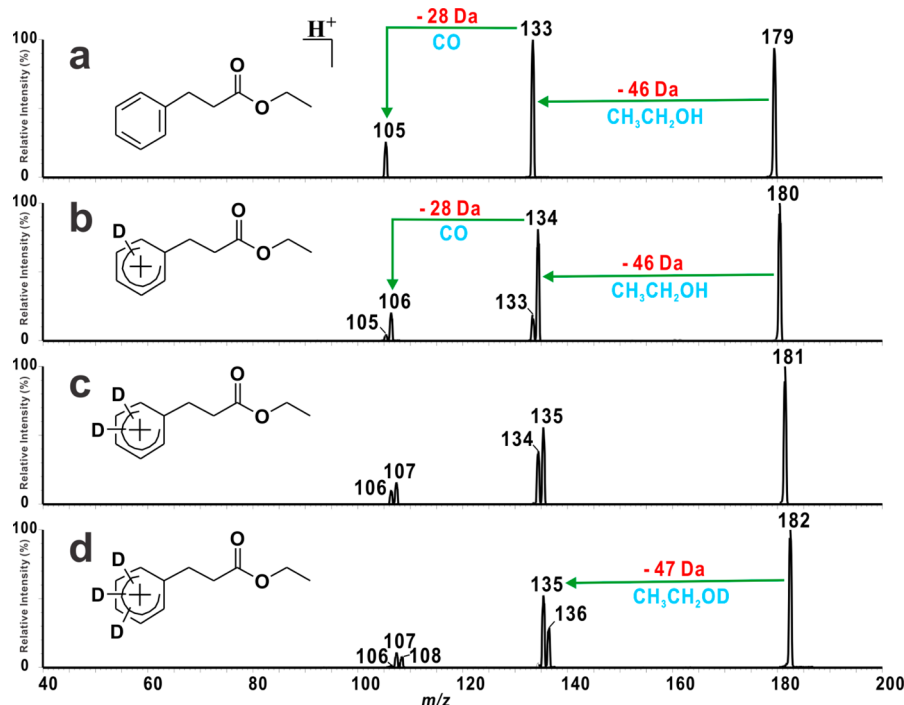


**Figure 8.** Product-ion spectrum of  $[M + H]^+$  ion of  $m/z$  179 ion of ethyl dihydrocinnamate (a), and those of  $m/z$  180 (b),  $m/z$  181 (c), and  $m/z$  182 (d) ions for the *mono*-, *di*-, and *tri*-deutero isotopologues generated by D/H exchange with  $D_2O$  in a HePI source (collision energy = 7 eV).

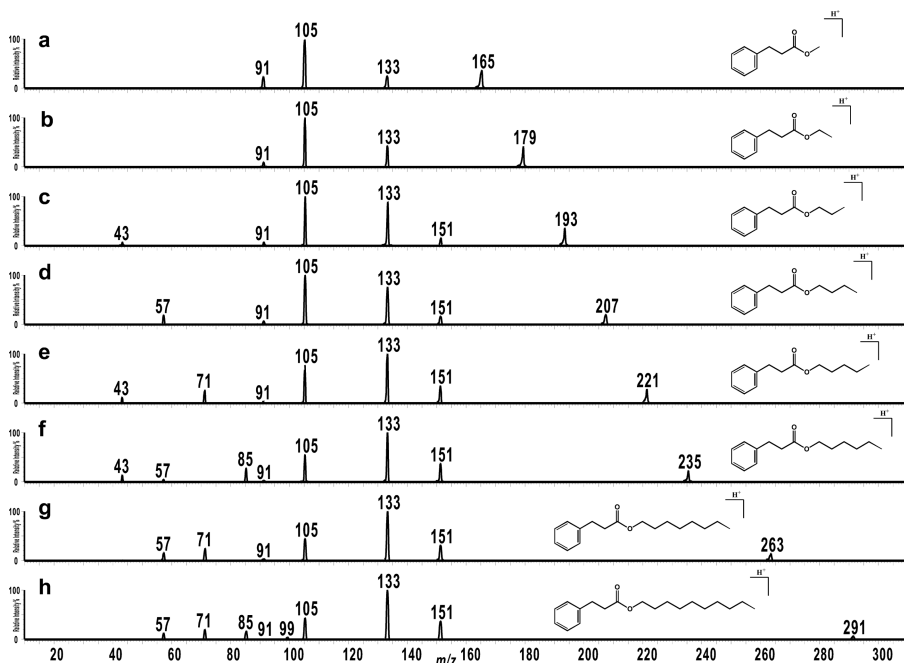


**Figure 9.** Product-ion spectra of  $m/z$  165, 179, 193, 207, 221, 235, 263, and 291 ions generated from protonated methyl (a), ethyl (b), *n*-propyl (c), *n*-butyl (d), *n*-pentyl (e), *n*-hexyl (f), *n*-octyl (g), and *n*-decyl (h) dihydrocinnamates, respectively. The spectra were recorded at a collision energy setting of 17 eV.

competition is between the processes that eliminate butene or butanol. Although a butene loss is common to all four isomers, it is most prominent for the *tert*-butyl isomer. Evidently, for the protonated *tert*-butyl ester, which requires the lowest degree of activation to initiate fragmentation, the isobutene elimination takes precedence over the *tert*-butanol loss. In contrast, a butene loss is less favorable for the protonated *n*-butyl ester because the initial primary carbocation, after the formation of the INC, has to

undergo several rearrangement steps before it is poised in the proper configuration for the proton transfer.

An examination of spectra recorded from protonated pentyl, hexyl, octyl, and decyl esters revealed that the alkene loss becomes a major fragmentation pathway as the size of the alkoxy group increases (Figure 9). However, a peak for the intact carbocation was not observed when the alkoxy group bears more than 7–8 carbon atoms (Figure 9) owing to the fact that the

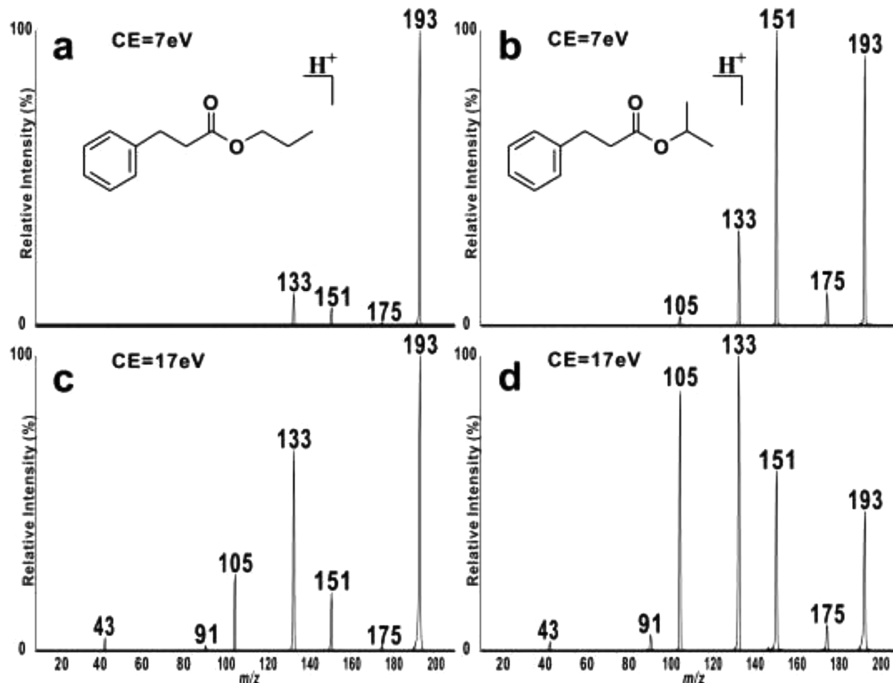


**Figure 10.** Product-ion spectra recorded from the  $m/z$  193  $[M + H]^+$  ion generated from *n*-propyl (a, c), and isopropyl (b, d) dihydrocinnamate, recorded at a collision energy setting of 7 eV (a, b) and 17 eV(c, d), respectively (all other parameters, including collision gas pressure and skimmer voltage, were identical).

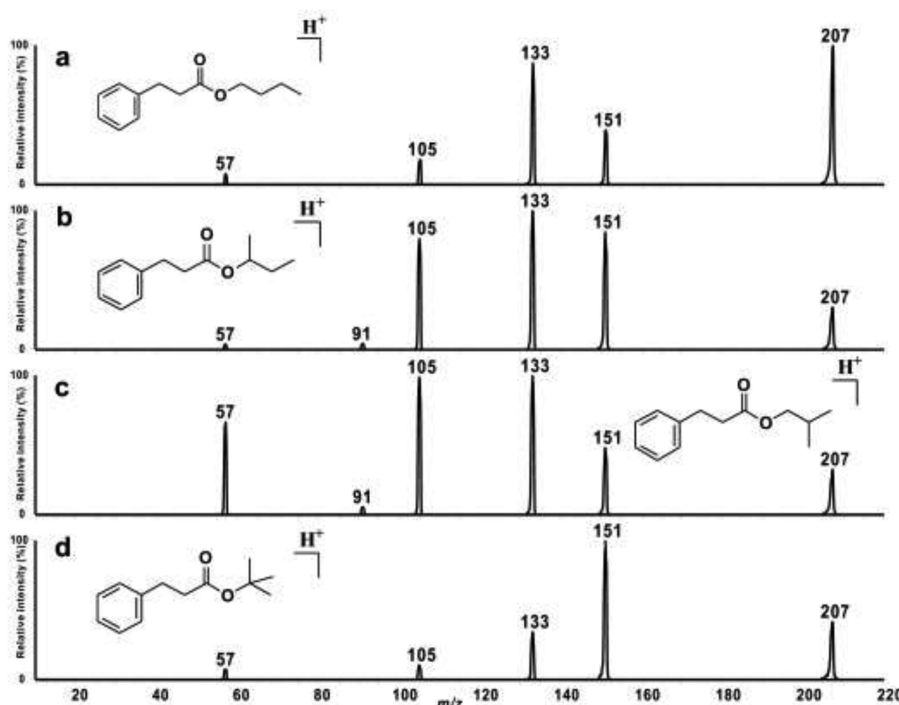
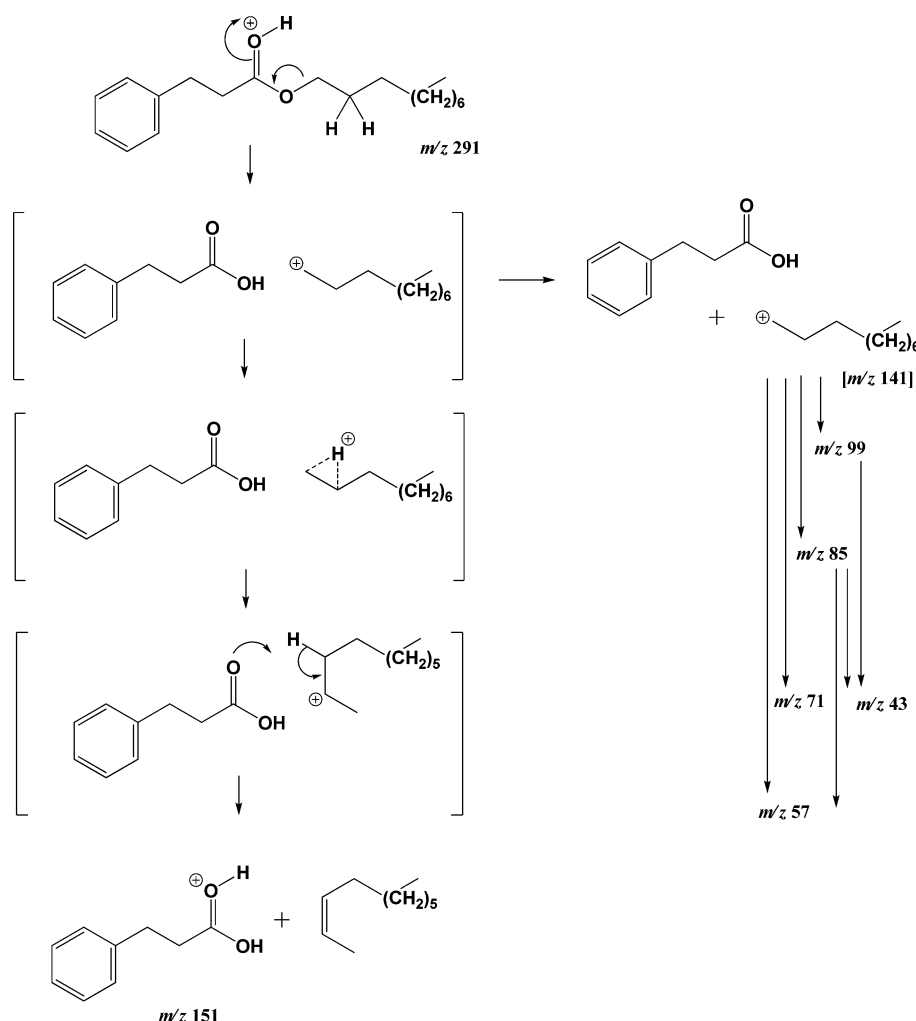


**Figure 11.** Product-ion spectra  $m/z$  207  $[M + H]^+$  ion generated from *n*-butyl (a), *sec*-butyl (b), isobutyl (c), and *tert*-butyl dihydrocinnamates (d), respectively. The spectra were recorded at a collision energy setting of 17 eV.

energy released by the rearrangements of the initial primary carbonium ion (or a proton-bridged nonclassical cation) within the INC, to form a more stable secondary or tertiary carbocation, is not dissipated to the surroundings because of the low pressure in the collision cell. Thus, the rearrangements render the product ions to be vibrationally more activated. In other words, because the mean-free path of ions and molecules is so large, there are no

collisions to accept the released energy. Consequently, the energy is not released: it undergoes internalization to vibrational modes and provides the impetus for the ions to undergo immediate dissociation to smaller and more stable carbonium ions by eliminating an alkene or a cycloalkane molecule (some of the reactions anticipated in this cascade of events are illustrated

**Scheme 3.** A Representation of the Cascade of Fragmentation Mechanisms that Protonated Decyl Dihydrocinnamate Undergoes upon Activation



in Scheme 3). The formation of smaller carbocations in a similar manner has been noted from protonated *N*-alkyl sulfonamides.<sup>22</sup>

To obtain support for the postulated cascade of events (Scheme 3), *n*-[1,1-<sup>2</sup>H]<sub>2</sub>decyl, *n*-[3,3-<sup>2</sup>H]<sub>2</sub>decyl, *n*-[4,4-<sup>2</sup>H]<sub>2</sub>-decyl, and *n*-[5,5-<sup>2</sup>H]<sub>2</sub>decyl dihydrocinnamate were synthesized and their product-ion spectra were recorded (Figure 12). Although the CID spectra of protonated *n*-dideuteriodecyl dihydrocinnamates bearing two deuterium atoms at carbon 1, 3, 4, or 5 positions were somewhat similar to each other, there were distinctive differences, particularly in the low-mass region. The results suggested that the ion for the peak at *m/z* 151, which represents protonated dihydrocinnamic acid, does not originate from a direct loss of a decene molecule from the precursor ion by a McLafferty-type mechanism (see the spectrum of protonated *n*-[2,2-<sup>2</sup>H]<sub>2</sub>octyl dihydrocinnamate in Supporting Information Figure S7, which confirmed that proton transfer does not take place specifically from the  $\gamma$  position as expected by a McLafferty-type mechanism<sup>24,25</sup>). We propose that the protonated dihydrocinnamate molecule fragments by a heterolytic cleavage of the O-CH<sub>2</sub> bond of the ester moiety to form an ion/neutral complex between dihydrocinnamic acid and a decyl carbocation ion (Scheme 3). Within an ion/neutral complex, the two members are held together only by electrostatic attractive forces. It is known that primary carbocation ions are short-lived in the gas

phase.<sup>23</sup> Thus, the decyl cation isomerizes very rapidly within the complex to more stable secondary or tertiary cations by 1,2-hydride shifts. In this way, the positional integrity of hydrogen atoms in the carbon chain is lost.<sup>26</sup> Consequently, the protonated dihydrocinnamic acid (*m/z* 151) formed by the alkene elimination acquires only a fraction of the deuterium labeling from any of the double-deuterium labeled alkyl groups in the dihydrocinnamates. If the carbocation underwent total scrambling before the final proton transfer occurs, then the ratio of the intensities of the *m/z* 151 and 152 peaks should be the same for all the [<sup>2</sup>H<sub>2</sub>]-isotopologues. However, Figure 12 shows that the intensity of the *m/z* 152 peak is distinctly higher in the spectra of the esters synthesized from *n*-[3,3-<sup>2</sup>H]<sub>2</sub>decanol and *n*-[4,4-<sup>2</sup>H]<sub>2</sub>-decanol (Figure 12c and 12d), which indicated that the proton transfer rate is higher than the scrambling rate.

In summary, the spectrum recorded from protonated *n*-decyl dihydrocinnamate does not show a peak at *m/z* 141 for the decyl cation itself, but it shows a series of peaks at *m/z* 43, 57, 71, 85, and 99 for smaller carbocations (Figure 12a). We propose that the decyl cation undergoes a rapid cascade of fast isomerizations and alkene eliminations before a proton is transferred to dihydrocinnamic acid within the complex. In the spectra of *n*-[<sup>2</sup>H<sub>2</sub>]<sub>2</sub>decyl dihydrocinnamates, all the peaks for the smaller carbocations appear as multiplets indicating that “scrambling”

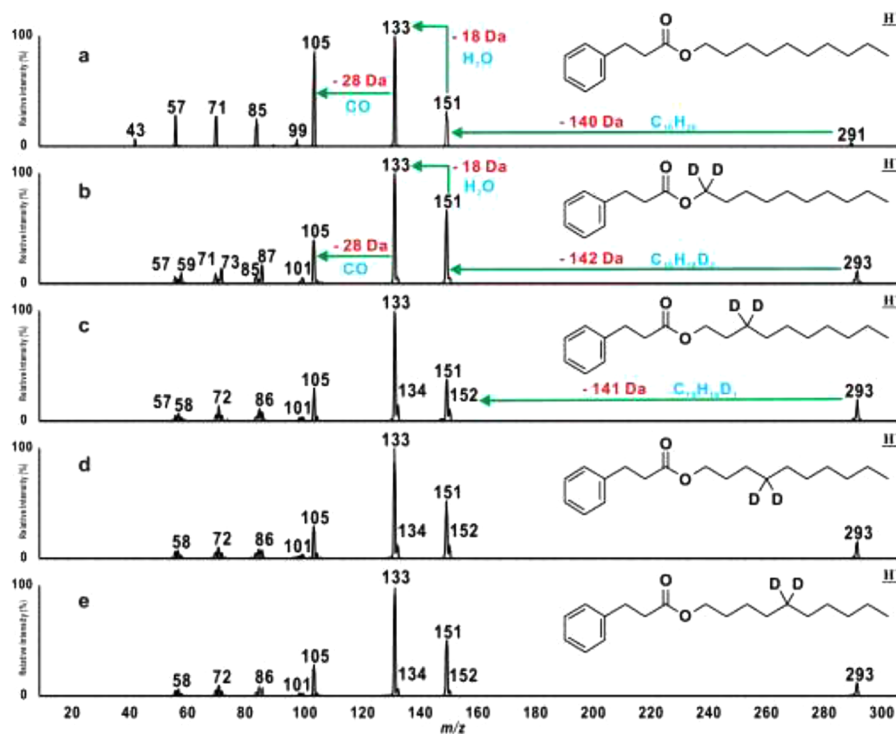


**Figure 12.** Product-ion spectra of the  $m/z$  291 [ $M + H$ ]<sup>+</sup> ion of *n*-decyl dihydrocinnamate (a),  $m/z$  293 [ $M + H$ ]<sup>+</sup> ion of *n*-[1,1-<sup>2</sup>H<sub>2</sub>]decyl dihydrocinnamate (b),  $m/z$  293 [ $M + H$ ]<sup>+</sup> ion of *n*-[3,3-<sup>2</sup>H<sub>2</sub>]decyl dihydrocinnamate (c),  $m/z$  293 [ $M + H$ ]<sup>+</sup> ion of *n*-[4,4-<sup>2</sup>H<sub>2</sub>]decyl dihydrocinnamate (d), and  $m/z$  293 [ $M + H$ ]<sup>+</sup> ion of *n*-[5,5-<sup>2</sup>H<sub>2</sub>]decyl dihydrocinnamate (e), recorded at a collision energy setting of 17 eV.

has taken place in the initial precursor carbocation as predicted by the proposed mechanism (**Scheme 3**; **Figure 12**). Similar mechanisms have been postulated previously for the fragmentation of protonated *p*-toluenesulfonamides synthesized from aliphatic amines.<sup>22</sup>

## CONCLUSIONS

Upon activation, protonated dihydrocinnamate esters in the gas-phase dissociate primarily by two fragmentation pathways. In one pathway, the alkoxy moiety is eliminated as an alkanol to generate protonated dihydrocinnamic acid ( $m/z$  151). For this pathway, the incipient proton (initially attached to the carbonyl oxygen) ambulates to the phenyl ring and then relocates to the alkoxy group to be eliminated as an alcohol. In the second pathway, the carbon–oxygen bond of the alkoxy group dissociates to form an ion-neutral complex (INC) between the alkyl cation and dihydrocinnamic acid. Within the complex, the alkyl cation rapidly rearranges by a cascade of hydride migrations and eventually transfers a proton to dihydrocinnamic acid to form an alkene.

## EXPERIMENTAL SECTION

**Chemicals.** Methanol-*d*<sub>3</sub>, D<sub>2</sub>O (99.9 atom % D), and H<sub>2</sub><sup>18</sup>O (95 atom % <sup>18</sup>O) were used as purchased from commercial suppliers.

**NMR Spectroscopy.** The structures of all synthetic products were confirmed by <sup>1</sup>H NMR. NMR spectra were recorded on a 400 MHz spectrometer (400 MHz for <sup>1</sup>H). Chemical shifts ( $\delta$ ) are reported in parts per million with tetramethylsilane, or the solvent resonance, as the internal standard. Coupling constants ( $J$ ) are given in hertz (Hz). Multiplicities are classified as follows: s, singlet; d, doublet; t, triplet; q, quartet; sept, septet; m, multiplet.

**Mass Spectrometry.** EI mass spectra (70 eV) were recorded by GC-MS. Collision-induced dissociation (CID) mass spectra were recorded on a triple-quadrupole tandem mass spectrometer equipped

with a HePI source.<sup>4</sup> A stream (~30 mL min<sup>-1</sup>) of high-purity helium (99.999%) was passed through the metal capillary held typically at about 3.5 kV. The source temperature was held at 100 °C. The hot (100 °C) desolvation gas (N<sub>2</sub>), at a flow of 90 L/h, was used to heat samples. Typically, the cone voltage of the ion source was set at 10 V. For CID experiments, the pressure of the argon in the collision cell was held around  $1.75 \times 10^{-4}$  mbar, and laboratory-frame collision energy was kept at about 25 eV, unless otherwise stated.

**Sample Introduction.** Liquid samples (1–5  $\mu$ L) were impregnated on silica gel (200  $\mu$ m; 5 mg) inside a glass capillary sealed on one side (1.5 cm; 1.5 mm ID). Each capillary was attached to the inner side of the cylindrical glass enclosure of the ion source with the aid of a small wad of “museum putty.” Most analyses were carried out under ambient conditions. For D/H exchange experiments, a cotton swab soaked in D<sub>2</sub>O was inserted to the enclosed source.<sup>3</sup>

**General Esterification Procedure.** Dihydrocinnamic acid (300 mg, 2.00 mmol) was mixed with methanol (64 mg, 2.00 mmol), ethanol (92 mg, 2.00 mmol), *n*-propanol (120 mg, 2.00 mmol), isopropanol (120 mg, 2.00 mmol), *n*-butanol (148 mg, 2.00 mmol), *sec*-butanol (148 mg, 2.00 mmol), isobutanol (148 mg, 2.00 mmol), *tert*-butanol (148 mg, 2.00 mmol), *n*-pentanol (176 mg, 2.00 mmol), *n*-hexanol (204 mg, 2.00 mmol), *n*-octanol (280 mg, 2.00 mmol), *n*-decanol (316 mg, 2.00 mmol), *n*-[1,1-<sup>2</sup>H<sub>2</sub>]decanol (316 mg, 2.00 mmol), *n*-[3,3-<sup>2</sup>H<sub>2</sub>]decanol (316 mg, 2.00 mmol), *n*-[4,4-<sup>2</sup>H<sub>2</sub>]decanol (316 mg, 2.00 mmol), or *n*-[5,5-<sup>2</sup>H<sub>2</sub>]decanol (316 mg, 2.00 mmol). A small amount of *p*-toluenesulfonic acid (25 mg, 0.15 mmol) was added, and the mixture was kept at room temperature. After 30 min, water (500  $\mu$ L) and diethyl ether (300  $\mu$ L) were added. The upper layer was separated, and the solvent was evaporated to obtain the product as oil. The residue was analyzed by HePI and GC-MS.

**Methyl Dihydrocinnamate.** EI-MS:  $m/z$  (%), 164 [ $M^{+•}$ , 34], 133 (8), 105 (32), 104 (100), 103 (14), 91 (48), 79 (10), 78 (13), 77 (20), 65 (9), 51 (10).

**Ethyl Dihydrocinnamate.** EI-MS:  $m/z$  (%), 178 [ $M^{+•}$ , 37], 133 (12), 107 (40), 105 (43), 104 (100), 91 (50), 79 (19), 78 (16), 77 (25), 65 (10), 51 (14).

*n*-Propyl Dihydrocinnamate. EI-MS:  $m/z$  (%), 192 [ $M^{+}$ , 36], 133 (20), 107 (37), 105 (44), 104 (100), 103 (16), 91 (63), 79 (16), 78 (16), 77 (24), 65 (11), 51 (13).

*Isopropyl Dihydrocinnamate*. EI-MS:  $m/z$  (%), 192 [ $M^{+}$ , 20], 150 (43), 133 (26), 105 (58), 104 (100), 103 (17), 91 (74), 79 (16), 78 (18), 77 (28), 65 (11), 51 (15), 43 (30).

*n-Butyl Dihydrocinnamate*. EI-MS:  $m/z$  (%), 206 [ $M^{+}$ , 27], 150 (18), 133 (11), 107 (25), 105 (37), 104 (100), 103 (13), 91 (60), 79 (12), 78 (13), 77 (19), 41 (16);  $^1\text{H}$  NMR (400 MHz,  $\text{CDCl}_3$ )  $\delta\text{H}$  1.07 (8H, t,  $J$  = 7.38,  $\text{CH}_3$ ), 1.50 (5H, m,  $\text{CH}_2$ ), 1.74 (6H, m,  $\text{CH}_2$ ), 2.78 (6H, m,  $\text{CH}_2$ ), 3.11 (6H, t,  $J$  = 7.91,  $\text{CH}_2$ ), 4.23 (5H, t,  $J$  = 6.66,  $\text{CH}_2$ ), 7.35 (8H, m, H-2,4,6), 7.44 (6H, m, H-3,5).

*sec-Butyl Dihydrocinnamate*. EI-MS:  $m/z$  (%), 206 [ $M^{+}$ , 9], 150 (59), 133 (39), 107 (14), 105 (62), 104 (100), 103 (16), 91 (78), 79 (14), 78 (16), 77 (24), 51 (14), 41 (18);  $^1\text{H}$  NMR (400 MHz,  $\text{CDCl}_3$ )  $\delta\text{H}$  1.01 (7H, t,  $J$  = 7.45,  $\text{CH}_3$ ), 1.32 (7H, d,  $J$  = 6.25,  $\text{CH}_3$ ), 1.69 (4H, m,  $\text{CH}_2$ ), 2.76 (5H, m,  $\text{CH}_2$ ), 3.11 (6H, t,  $J$  = 7.75,  $\text{CH}_2$ ), 4.99 (1H, s, CH), 5.00 (1H, d,  $J$  = 6.25), 7.36 (9H, m, H-2,4,6), 7.43 (7H, m, H-3,5).

*Isobutyl Dihydrocinnamate*. EI-MS:  $m/z$  (%), 206 [ $M^{+}$ , 22], 150 (41), 133 (25), 107 (18), 105 (54), 104 (100), 103 (17), 91 (77), 79 (16), 78 (17), 77 (25), 57 (25), 41 (26);  $^1\text{H}$  NMR (400 MHz,  $\text{CDCl}_3$ )  $\delta\text{H}$  1.07 (4H, m,  $\text{CH}_3$ ), 1.07 (12H, d,  $J$  = 6.78,  $\text{CH}_3$ ), 2.06 (2H, m, CH), 2.83 (6H, m,  $\text{CH}_2$ ), 3.12 (6H, m,  $\text{CH}_2$ ), 4.02 (5H, d,  $J$  = 6.70,  $\text{CH}_2$ ), 7.37 (9H, m, H-2,4,6), 7.45 (6H, m, H-3,5).

*tert-Butyl Dihydrocinnamate*. EI-MS:  $m/z$  (%), 105 (21), 104 (30), 103 (21), 91 (29), 79 (14), 78 (23), 77 (35), 58 (11), 57 (80), 51 (26), 43 (100), 42 (23), 41 (64), 39 (54), 59 (36);  $^1\text{H}$  NMR (400 MHz,  $\text{CDCl}_3$ )  $\delta\text{H}$  1.57 (16H, m,  $\text{CH}_3$ ), 2.69 (6H, m,  $\text{CH}_2$ ), 3.06 (6H, m,  $\text{CH}_2$ ), 7.36 (6H, m, H-2,4,6), 7.41 (10H, m, H-3,5).

*n-Pentyl Dihydrocinnamate*. EI-MS:  $m/z$  (%), 220 [ $M^{+}$ , 5], 150 (14), 133 (5), 107 (18), 105 (38), 104 (100), 103 (19), 91 (85), 79 (18), 78 (24), 77 (33), 65 (18), 51 (23), 43 (76).

*n-Hexyl Dihydrocinnamate*. EI-MS:  $m/z$  (%), 234 [ $M^{+}$ , 18], 150 (36), 133 (8), 105 (34), 104 (100), 103 (10), 91 (55), 79 (10), 78 (10), 77 (15), 43 (23), 41 (19).

*n-Octyl Dihydrocinnamate*. EI-MS:  $m/z$  (%), 262 [ $M^{+}$ , 13], 150 (53), 133 (8), 105 (34), 104 (100), 103 (9), 91 (53), 79 (9), 78 (9), 77 (12), 57 (16), 43 (21), 41 (26).

*n-Decyl Dihydrocinnamate*. EI-MS:  $m/z$  (%), 290 [ $M^{+}$ , 12], 150 (70), 133 (10), 107 (13), 105 (36), 104 (100), 91 (49), 77 (11), 57 (17), 55 (17), 43 (30), 41 (30).

*n-[1-<sup>2</sup>H]Decyl Dihydrocinnamate*. EI-MS:  $m/z$  (%), 292 [ $M^{+}$ , 1], 150 (12), 133 (3), 105 (24), 104 (69), 91 (51), 79 (11), 78 (11), 77 (13), 71 (13), 59 (22), 58 (13), 57 (46), 56 (16), 55 (26), 45 (20), 44 (23), 43 (100), 42 (31), 41 (67), 39 (15).

*n-[3,3-<sup>2</sup>H]Decyl Dihydrocinnamate*. EI-MS:  $m/z$  (%), 292 [ $M^{+}$ , 1], 150 (12), 133 (3), 105 (33), 104 (75), 91 (59), 79 (13), 78 (11), 77 (15), 72 (12), 71 (12), 59 (15), 58 (34), 57 (42), 56 (24), 55 (22), 45 (17), 44 (44), 43 (100), 42 (38), 41 (64), 39 (16).

*n-[4,4-<sup>2</sup>H]Decyl Dihydrocinnamate*. EI-MS:  $m/z$  (%), 292 [ $M^{+}$ , 1], 150 (16), 133 (5), 107 (14), 105 (42), 104 (100), 92 (10), 91 (73), 86 (10), 79 (15), 78 (14), 77 (18), 72 (15), 71 (14), 65 (11), 59 (15), 58 (37), 57 (44), 56 (25), 55 (19), 51 (10), 45 (14), 43 (90), 42 (37), 41 (56), 39 (14).

*n-[5,5-<sup>2</sup>H]Decyl Dihydrocinnamate*. EI-MS:  $m/z$  (%), 292 [ $M^{+}$ , 1], 150 (19), 133 (5), 107 (14), 105 (40), 104 (100), 103 (11), 91 (69), 79 (12), 78 (12), 77 (15), 72 (13), 71 (11), 59 (11), 58 (29), 57 (31), 56 (18), 55 (16), 45 (12), 44 (35), 43 (60), 42 (27), 41 (40), 39 (10).

[Carbonyl-<sup>18</sup>O]Dihydrocinnamic acid. To a solution of dihydrocinnamic acid (300 mg, 2.00 mmol) in THF (0.5 mL),  $\text{H}_2^{18}\text{O}$  (about 100  $\mu\text{L}$ ) and concentrated sulfuric acid (5  $\mu\text{L}$ ) were added and the mixture was kept at room temperature (20 °C). After 30 min, THF was removed and the residue was dried with a stream of dry nitrogen to give [carbonyl-<sup>18</sup>O]dihydrocinnamic acid. EI-MS:  $m/z$  (%), 104 (60), 91 (100), 79 (9), 77 (16), 65 (10), 51 (14).

*Methyl, Ethyl, and n-Butyl [Carbonyl-<sup>18</sup>O]dihydrocinnamates*. Absolute methanol (64 mg, 2.00 mmol), ethanol (92 mg, 2.00 mmol), or *n*-butanol (148 mg, 2.00 mmol) and *p*-toluenesulfonic acid (25 mg, 0.15 mmol) were added to [carbonyl-<sup>18</sup>O]dihydrocinnamic acid (300 mg, 2.00 mmol). The mixture was kept at room temperature for 30 min,

and water (500  $\mu\text{L}$ ) and diethyl ether (300  $\mu\text{L}$ ) were added. The upper layer was separated, and the solvent was evaporated to obtain the product as an oil.

*Methyl [Carbonyl-<sup>18</sup>O]dihydrocinnamate*. EI-MS:  $m/z$  (%), 166 [ $M^{+}$ , 34], 135 (8), 105 (32), 104 (100), 103 (14), 91 (48), 79 (10), 78 (13), 77 (20), 65 (9), 51 (10).

*Ethyl [Carbonyl-<sup>18</sup>O]dihydrocinnamate*. EI-MS:  $m/z$  (%), 180 [ $M^{+}$ , 37], 135 (10), 107 (40), 105 (42), 104 (100), 91 (50), 79 (20), 77 (25), 65 (10), 51 (14).

*n-Butyl [Carbonyl-<sup>18</sup>O]dihydrocinnamate*. EI-MS:  $m/z$  (%), 208 [ $M^{+}$ , 24], 152 (19), 133 (11), 105 (37), 104 (100), 91 (60), 79 (15), 78 (14), 77 (23), 41 (19).

[2,2-<sup>2</sup>H]Heptanenitrile. Heptanenitrile (500  $\mu\text{L}$ ) was added to a mixture of  $\text{D}_2\text{O}$ /dioxane (7:2) (2 mL) and diazabicyclo[5.4.0]undec-7-ene (DBU, 1 mL). The mixture was heated at 100 °C for 2 h, and the solvent was removed under reduced pressure. After four repetitions of the D/H procedure, the residue was washed with aqueous HCl and the product was extracted into diethyl ether. EI-MS:  $m/z$  (%), 113 [ $M^{+}$ , 5], 112 (3), 99 (11), 98 (27), 97 (19), 85 (25), 84 (66), 83 (39), 82 (12), 71 (17), 70 (14), 57 (14), 56 (18), 54 (20), 53 (13), 43 (66), 42 (46), 41 (100), 40 (22).

[2,2-<sup>2</sup>H]Octanoic Acid. Hydrochloric acid (1.0 mL) was added to [2,2-<sup>2</sup>H]heptanenitrile (300  $\mu\text{L}$ ), and the mixture was kept at 100 °C. After 6 h, the product was isolated under reduced pressure as a white solid. EI-MS:  $m/z$  (%), 87 (28), 74 (100), 59 (24), 57 (21), 55 (33), 43 (62), 42 (21), 41 (53), 39 (24).

[2,2-<sup>2</sup>H]Octanol. LiAlH<sub>4</sub> in THF (200  $\mu\text{L}$ ) was slowly added to [2,2-<sup>2</sup>H]octanoic acid at room temperature. After 15 min, water (350  $\mu\text{L}$ ) was added to the mixture. The upper layer was separated, and the product was evaporated as an oil.

[2,2-<sup>2</sup>H]Octyl Dihydrocinnamate. Dihydrocinnamic acid (300 mg, 2.00 mmol) and *p*-toluenesulfonic acid (25 mg, 0.15 mmol) were added to [2,2-<sup>2</sup>H]octanol at room temperature. After 30 min, water (500  $\mu\text{L}$ ) and diethyl ether (300  $\mu\text{L}$ ) were added. The upper layer was separated, and the product was evaporated as an oil. EI-MS:  $m/z$  (%), 264 [ $M^{+}$ , 10], 150 (21), 133 (12), 107 (37), 104 (100), 91 (63), 79 (5), 78 (9), 77 (13), 59 (20), 58 (17), 57 (14), 45 (21), 44 (35), 43 (12), 42 (20).

[2,2,3,3-<sup>2</sup>H<sub>4</sub>]Dihydrocinnamic Acid. Phenylpropionic acid (0.1 g, 0.68 mmol) was added to 10% Pd/C (10.0 mg) in ethyl acetate (2.0 mL). Deuterium gas was infused into the solution at room temperature. After 12 h, the mixture was filtered and the filtrate was concentrated to obtain the desired compound as a white solid (85 mg, 81%). EI-MS:  $m/z$  (%), 154 [ $M^{+}$ , 22], 107 (44), 106 (48), 105 (34), 93 (72), 92 (100), 91 (40).

*Methyl [2,2,3,3-<sup>2</sup>H<sub>4</sub>]Dihydrocinnamate*. [2,2,3,3-<sup>2</sup>H<sub>4</sub>]Dihydrocinnamic acid (15.0 mg, 0.09 mmol) and *p*-toluenesulfonic acid (1.0 mg) were added to methanol (0.5 mL) at room temperature. The mixture was stirred for 12 h, and the solvent was removed under reduced pressure. The residue was washed with ethyl acetate (5.0 mL), NaHCO<sub>3</sub> solution (5.0 mL), and water (5.0 mL). The upper layer was separated and dried with Na<sub>2</sub>SO<sub>4</sub>, and the solvent was removed to obtain the product as a colorless oil (8.0 mg, 50%). EI-MS:  $m/z$  (%), 168 [ $M^{+}$ , 32], 137 (8), 107 (100), 93 (88), 79 (33), 66 (12), 51 (25).

**Computational Methods.** Full geometry optimizations were performed by the density functional theory method B3LYP with a 6-311++G(2d,2p) basis set for all atoms using the Gaussian 09 program,<sup>28</sup> which was also used to calculate the zero-point-energy-corrected electronic energies, enthalpies, and Gibbs free energies. The latter two calculations were performed at 298.15 K and 1 atm, as standard output from the Gaussian 09 program. Frequency analysis was undertaken at the same level to confirm that the optimized structures are the corresponding stationary states on the respective potential energy surfaces.

## ASSOCIATED CONTENT

### Supporting Information

The Supporting Information is available free of charge on the ACS Publications website at DOI: [10.1021/acs.joc.Sb01390](https://doi.org/10.1021/acs.joc.Sb01390).

Product ion spectra of protonated ethyl, *n*-propyl, isopropyl, *n*-butyl, and *n*-octyl dihydrocinnamate, and that of methyl [2,2,3,3-<sup>2</sup>H<sub>4</sub>]dihydrocinnamate, and atom coordinates and absolute energies of structures in Figures 5 (PDF)

## AUTHOR INFORMATION

### Corresponding Author

\*E-mail: athula.attygalle@stevens.edu.

### Notes

The authors declare no competing financial interest.

## ACKNOWLEDGMENTS

This research was supported by funds provided by Stevens Institute of Technology (Hoboken, NJ). We thank Bristol-Myers Squibb (New Brunswick, NJ) for the donation of the triple quadrupole mass spectrometer.

## REFERENCES

- (1) Korneev, S. M. *Synthesis* **2013**, *45*, 1000–1015.
- (2) Yang, Z.; Pavlov, J.; Attygalle, A. B. *J. Mass Spectrom.* **2012**, *47*, 845–852.
- (3) Attygalle, A. B.; Gangam, R.; Pavlov, J. *Anal. Chem.* **2014**, *86*, 928–935.
- (4) Cody, R. B.; Laramée, J. A.; Durst, H. D. *Anal. Chem.* **2005**, *77*, 2297–2302.
- (5) Herman, J. A.; Harrison, A. G. *Can. J. Chem.* **1981**, *59*, 2133–2145.
- (6) Komáromi, I.; Somogyi, Á.; Wysocki, V. H. *Int. J. Mass Spectrom.* **2005**, *241*, 315–323.
- (7) Vaisar, T. In *Encyclopedia of Mass Spectrometry*. Vol. 4, *Fundamentals of and Applications to Organic (and Organometallic) Compounds*; Nibbering, N. M. M., Ed.; Elsevier: Amsterdam, 2005; Vol. 4, pp 752–762.
- (8) Kuck, D.; Petersen, A.; Fastabend, U. *Int. J. Mass Spectrom.* **1998**, *179-180*, 129–146.
- (9) For the relative sum of electronic and thermal enthalpies, see Supporting Information Table T1.
- (10) For atom coordinates and absolute energies of structures in Figures 5, see Supporting Information Table T2.
- (11) Freiser, B. S.; Woodin, R. L.; Beauchamp, J. L. *J. Am. Chem. Soc.* **1975**, *97*, 6893–6894.
- (12) Kuck, D. *Int. J. Mass Spectrom.* **2002**, *213*, 101–144.
- (13) Chiavarino, B.; Crestoni, M. E.; Di Renzo, B.; Fornarini, S. *J. Am. Chem. Soc.* **1998**, *120*, 10856–10862.
- (14) Ni, J.; Harrison, A. G. *Can. J. Chem.* **1995**, *73*, 1779–1784.
- (15) The conversion of intermediate 2→3 is a trivial rotation, thus finding a TS<sub>2-3</sub> was not sought.
- (16) Numerous efforts to locate a structure for TS<sub>3-4</sub> were unsuccessful. All attempts converged to a structure similar to 4, which suggested that once the proton is transferred, the intermediate 3 rapidly transforms to species 4.
- (17) Nibbering, N. M. M.; Nishishita, T.; Van de Sande, C. C.; McLafferty, F. W. *J. Am. Chem. Soc.* **1974**, *96*, 5668–5669.
- (18) Olah, G. A.; Porter, R. D. *J. Am. Chem. Soc.* **1971**, *93*, 6877–6887.
- (19) Veith, H. J.; Gross, J. H. *Org. Mass Spectrom.* **1991**, *26*, 1097–1108.
- (20) Bowen, R. D.; Colburn, A. W.; Derrick, P. J. *J. Chem. Soc., Perkin Trans. 2* **1991**, 147–151.
- (21) McAdoo, D. J.; Bowen, R. D. *Eur. Mass Spectrom.* **1999**, *5*, 389–409.
- (22) Bialecki, J. B.; Weisbecker, C. S.; Attygalle, A. B. *J. Am. Soc. Mass Spectrom.* **2014**, *25*, 1068–1078.
- (23) Bouchoux, G. *J. Mass Spectrom.* **2013**, *48*, 505–517.
- (24) Laulhé, S.; Bogdanov, B.; Johannes, L. M.; Gutierrez, O.; Harrison, J. G.; Tantillo, D. J.; Zhang, X.; Nantz, M. J. *J. Mass Spectrom.* **2012**, *47*, 676–686.
- (25) Tureček, F. In *Encyclopedia of Mass Spectrometry*. Vol. 4, *Fundamentals of and Applications to Organic (and Organometallic) Compounds*; Nibbering, N. M. M., Ed.; Elsevier: Amsterdam, 2005; Vol. 4, pp 396–403.
- (26) Kenny, D. V.; Olesik, S. V. *J. Am. Soc. Mass Spectrom.* **1994**, *5*, 544–552.
- (27) Ni, J.; Harrison, A. G. *Can. J. Chem.* **1995**, *73*, 1779–1784.
- (28) Frisch, M. J.; Trucks, G. W.; Schlegel, H. B.; Scuseria, G. E.; Robb, M. A.; Cheeseman, J. R.; Scalmani, G.; Barone, V.; Mennucci, B.; Petersson, G. A.; Nakatsuji, H.; Caricato, M.; Li, X.; Hratchian, H. P.; Izmaylov, A. F.; Bloino, J.; Zheng, G.; Sonnenberg, J. L.; Hada, M.; Ehara, M.; Toyota, K.; Fukuda, R.; Hasegawa, J.; Ishida, M.; Nakajima, T.; Honda, Y.; Kitao, O.; Nakai, H.; Vreven, T.; Montgomery, Jr., J. A.; Peralta, E.; Ogliaro, F.; Bearpark, M.; Heyd, J. J.; Brothers, E.; Kudin, K. N.; Staroverov, V. N.; Keith, T.; Kobayashi, R.; Normand, J.; Raghavachari, K.; Rendell, A.; Burant, J. C.; Iyengar, S. S.; Tomasi, J.; Cossi, M.; Rega, N.; Millam, J. M.; Klene, M.; Knox, J. E.; Cross, J. B.; Bakken, V.; Adamo, C.; Jaramillo, J.; Gomperts, R.; Stratmann, R. E.; Yazeyev, O.; Austin, A. J.; Cammi, R.; Pomelli, C.; Ochterski, J. W.; Martin, R. L.; Morokuma, K.; Zakrzewski, V. G.; Voth, G. A.; Salvador, P.; Dannenberg, J. J.; Dapprich, S.; Daniels, A. D.; Farkas, O.; Foresman, J. B.; Ortiz, J. V.; Cioslowski, J.; Fox, D. J. *Gaussian 09*, Revision D.01; Gaussian, Inc.: Wallingford, CT, 2013.